Available online at www.sciencedirect.com

ScienceDirect

Procedia CIRP 82 (2019) 326–331

www.elsevier.com/locate/procedia

17th CIRP Conference on Modelling of Machining Operations

On the surface integrity of Electron Beam Melted Ti6Al4V after machining

R. Bertolini[a]*, L. Lizzul[a], S. Bruschi[a], A. Ghiotti[a]

[a]*Department of Industrial Engineering, University of Padova, Via Venezia 1, 35131, Padova, Italy*

* Corresponding author. Tel.049-827 6819 *E-mail address:* rachele.bertolini@phd.unipd.it

Abstract

The Additive Manufacturing process known as Electron Beam Melting (EBM) is increasingly used to produce Ti6Al4V biomedical parts, whose functional surfaces, however, need to be machined afterwards. The paper addresses the fundamental issue of surface integrity of EBM parts when subjected to machining operation under dry, flood and cryogenic cooling conditions. The machined surface integrity is evaluated in terms of microstructural and mechanical features, residual stresses, surface topography and defects. Results are then compared to the outcomes of the same machining tests carried out on the conventional wrought alloy. This study points out the different machinability of the two investigated alloys, highlighting that new insights into optimization of parameters for machining AM alloys are needed.

Peer-review under responsibility of the scientific committee of The 17th CIRP Conference on Modelling of Machining Operations

Keywords: Surface integrity; Turning; Additive Manufacturing

1. Introduction

Additive Manufacturing (AM) is emerging as an innovative manufacturing technology and shows great potential in the biomedical field since it allows obtaining patient-specific components with improved biocompatibility [1]. Even if classified as a net-shape technology, some finishing machining operations may be still required on functional surfaces produced by AM. However, in literature there is a lack of studies about AM alloys machinability and surface integrity, especially when the AM technology known as Electron Beam Melting (EBM) is considered [2]. Particularly in advanced sectors as the biomedical one, the analysis of the machined surface integrity becomes compulsory to attempt predicting the in-service performances, the latter being greatly affected by the machining-induced mechanical and microstructural alterations [3].

In this scenario, the paper presents the evaluation of the EBM Ti6Al4V machinability in terms of surface integrity to be correlated to the alloy service life performances, such as corrosion resistance and fatigue life.

The Ti6Al4V alloy examined in this study is widely used for biomedical implants for which both fatigue and corrosion resistance are pivotal as these components are subjected to repeated loads in an aggressive environment [4,5]. The well-known low machinability of the wrought Ti6Al4V might be further reduced by the peculiar EBM microstructure, leading to an overall worsening of the machined surface integrity.

Semi-finishing turning operations were carried out under dry, flood and cryogenic conditions, as different cooling conditions may play a role in determining the machined surface integrity. The latter was investigated in terms of microstructural and mechanical alterations to assess the formation of a superficial deformed layer, the nano-hardness variations and the nature of residual stresses. Furthermore, the surface finish was evaluated by means of 3D surface analysis. For sake of comparison, also the results of the same machining tests carried out on the wrought Ti6Al4V are reported.

2212-8271
Peer-review under responsibility of the scientific committee of The 17th CIRP Conference on Modelling of Machining Operations
10.1016/j.procir.2019.04.166

2. Materials and methods

2.1. Material

The material under examination is the grade 5 titanium alloy (Ti6Al4V). The investigated samples were conventionally and additively manufactured, namely wrought and EBM titanium alloy samples were employed. The wrought material was supplied by Sandvik™ Bioline (annealed Ti6Al4V ELI bar) in form of bars of 50 mm of diameter. The AM material was produced using the ARCAM™ Q10 machine, with the built up direction along the longitudinal axis of the cylindrical samples.

The microstructures of the wrought and EBM Ti6Al4V are reported in Fig. 1 a) and b), respectively.

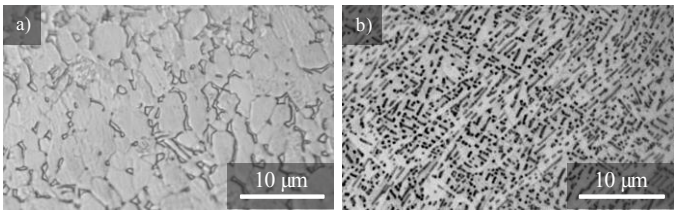

Fig. 1. Optical micrographs of the Ti6Al4V microstructure: a) wrought and b) EBM.

As expected, the wrought material is characterized by a globular microstructure distinctive of the annealing process. On the contrary, Fig. 1 b) shows for the EBM material a very fine acicular microstructure, which mainly consists of α-phase fine lamellae, organized in a basket weave morphology. The EBM Ti6Al4V presents higher Ultimate Tensile Strength (UTS), Yield Stress (YS) and elastic modulus than the conventional wrought alloy, whereas the elongation is slightly lower, as a consequence of the different microstructure (see Table 1).

Table 1. Mechanical properties of as-delivered alloys.

Material	Processing route	E (GPa)	UTS (MPa)	YS (MPa)	Elongation (%)
Ti6Al4V	Wrought*	114	860	790	15
Ti6Al4V	EBM**	120	1020	950	14

* Data are in accordance to those reported by [6].
**Data are in accordance to those reported by [7].

2.2. Machining tests

The machining trials were performed on a Mori Seiki™ NL 1500 CNC lathe equipped with a special designed apparatus for delivery of the cryogenic coolant. The CNMG120404-SM 1125 supplied by Sandvik-Coromant™ was used as cutting tool insert, suitable for machining titanium alloys. The cutting tool was mounted on a SandvikTM PLCNL 2020K 12 tool holder with an approach angle of 95°. In order to avoid the influence of the tool wear, a fresh cutting edge was adopted for each test.

Semi-finishing cutting operations were carried out with a depth of cut equal to 0.25 mm at a cutting speed of 80 m/min and feed of 0.1 mm/rev. Tests were performed under different cooling conditions, namely dry, flood and cryogenic. Dry condition refers to the machining operation in absence of any lubricant. Flood condition refers to the machining operation carried out with the use of an emulsion coolant, which was the standard commercial semi-synthetic cutting fluid Monroe™ Astro-Cut HD XBP mixed with water (1:20 mix ratio). Cryogenic condition refers to the machining operation carried out using liquid nitrogen as coolant, which was sprayed against the tool rake and flank faces at a constant pressure of 15 bars. Detailed information on the cryogenic equipment can be found in [8]. Table 2 summarizes the experimental conditions used in this study.

Table 2. Experimental plan for the machining tests.

Processing route	Cooling condition
Wrought	Dry
Wrought	Flood
Wrought	Cryogenic
EBM	Dry
EBM	Flood
EBM	Cryogenic

2.3. Microstructural and mechanical characterization

After machining, the Ti6Al4V cylinders were cut to prepare metallographic samples. The samples were hot mounted, ground using up to 4000 SiC grit paper, and then polished using 3 μm diamond paper and SiO_2 colloidal dispersion in demineralized water. The polished samples were cleaned in an acetone ultrasound bath for 15 min, then rinsed in demineralized water, and finally dried by compressed air. Kroll's solution was used as etchant to reveal the grain boundaries. The microstructure observations were conducted using a Leica™ DMRE optical microscope equipped with a high definition digital camera. To quantify the thickness of the affected layer, the extent of the deformed grains and lamellae was measured every 20 μm from optical microscope images at 1000× magnification, via the ImageJ program. The procedure was done in ten zones of each specimen and lastly, the mean value was determined.

Measurements of nano-hardness were carried out by means of the iMicro™ nano-indenter from Nanomechanics Inc. making use of a Berkovich diamond indenter. Indentations were performed with a load of 20 mN along a line composed by six points, starting approximately from a distance of 30 μm from the machined surface. The load was kept low enough in order to minimize the distance between two subsequent points and to appreciate differences between the samples. Measurements were performed on three different zones across the section of each sample.

The residual stresses on the samples surfaces were measured by means of the X-Ray Diffraction (XRD) technique via the sin2ψ method. The SpiderX™ portable diffractometer from GNR measured the residual stresses using CuKα radiation at 90 μA at 9 tilt angles (ψ). Both the axial and the tangential directions were scanned.

2.4. Surface finishing analysis

The Sensofar™ PLU-Neox optical profiler with a 20x Nikon™ confocal objective was used to scan the surface topography of the Ti6Al4V cylinders after machining.

Data processing, filtering and evaluation of the surface texture parameters were performed according to the ISO 25178 series [9]. Surface texture has been recognized to have a strong influence on fatigue life [10, 11] and corrosion resistance [12]. The most significant parameters to consider for such purpose are the following:

- Arithmetical mean height of the scale-limited surface (*Sa*), the most popular areal parameter, which represents the baseline for comparison with other research works.
- Reduced valley depth (*Svk*), a parameter that indicates the valley depth below the core roughness, effective in discriminating the presence of possible stress concentration sites or dales where a fluid can collect.
- Skewness of the scale-limited surface (*Ssk*), which refers to the symmetry of the profile about the mean line; it defines if a surface is dominated by peaks or valleys. This parameter relates well with porosity and load carrying ability.

To inspect surface defects, the FEI™ QUANTA 450 Scanning Electron Microscope (SEM) with the Backscattered Electron Detector (BSED) was utilized.

3. Experimental results

3.1. Microstructural and mechanical characterization of the machined workpieces

Fig. 2 reports the microstructure under the machined surfaces as a function of the investigated process parameters. A thin layer of altered material in which the grains are deformed along the cutting direction is visible, regardless of the processing route and lubrication condition adopted. It is worth noting that both the grain size and the lamellae thickness are smaller than those underneath the affected layer.

Even if the microstructure is altered compared to the as-received alloy (see Fig. 1), no phase transformation can be detected since the cutting temperature did not exceed the alloy beta-transus one, in dry machining as well.

More in detail, it was observed that the extension of the altered layer was slightly higher in the case of EBM alloy, compared to the wrought one. This can be due to the different mechanical properties related to the alloy processing route.

A clear trend related to the different cooling conditions could be identified, since in the case of cryogenic cooling the affected layer width was always higher than that one that pertained to dry and flood conditions. In fact, cryogenic cooling led to an increase of the altered layer thickness of approximately 31% and 44% compared to the dry condition in the case of wrought and EBM alloy, respectively.

The effect of the process parameters on nano-hardness profiles was investigated and results are shown in Fig. 3. The nano-hardness values were normalized with respect to the as-delivered condition that is 5.8 ± 0.19 GPa for the wrought condition, and 6.1 ± 0.28 GPa for the EBM one. Nano-hardness increased near the machined surface and gradually decreased as a function of the distance from the surface. Such increment can be attributed to the reduction of the grain size and the lamellae thickness paired with plastic deformation [13], which can be qualitatively appreciated in Fig. 2. An exception is represented by the first indentation that does not respect the general trend. This can be implied to the predominance of the relaxation phenomenon on the strain hardening one, due to the heat generated during machining process combined with the low thermal conductivity typical of titanium alloys [14].

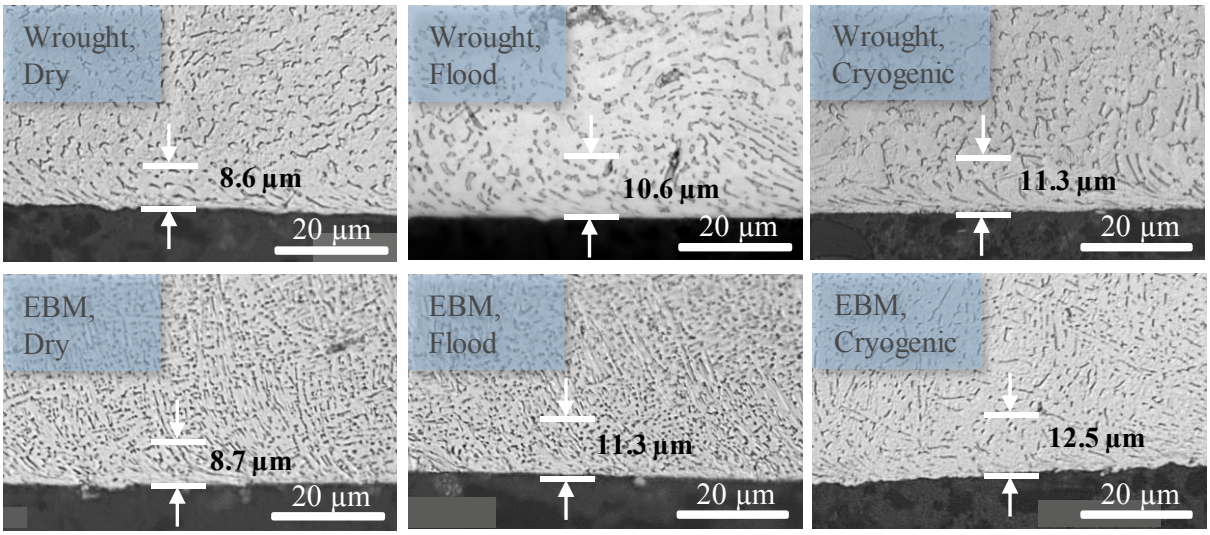

Figure 2. Microstructures under the machined surface as a function of the process parameters. Thickness values of the affected layer are displayed on the image (standard deviations less than 5%).

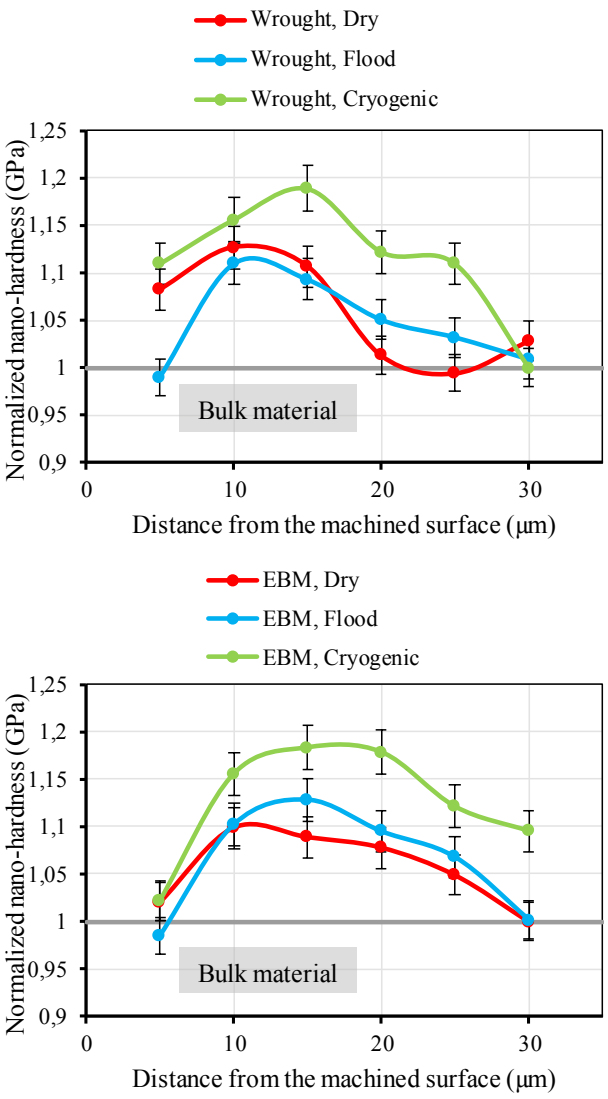

Figure 3. Normalized nano-hardness values under the machined surface as a function of the process parameters.

Table 3. Residual stresses at the machined surface along the axial direction (σa) and tangential direction (σt) as a function of the process parameters.

Processing route	Cooling condition	σa (MPa)	σt (MPa)
Wrought	Dry	-306 ± 6	-504 ± 18
Wrought	Flood	-386 ± 8	-584 ± 4
Wrought	Cryogenic	-456 ± 5	-863 ± 9
EBM	Dry	-351 ± 5	-356 ± 9
EBM	Flood	-403 ± 12	-500 ± 3
EBM	Cryogenic	-467 ± 4	-498 ± 4

The wrought and the EBM alloys were similarly affected by the machining process in terms of nano-hardness increase, even if, in the case of EBM alloy, a perceptible increment involved a wider material portion (up to 25 µm from the machined surface), whereas in the wrought samples the hardness started to decrease already at 15 µm. These results are in accordance to the trend found in the microstructural characterization confirming that EBM titanium samples are more sensible to machining-induced hardening, as highlighted in other studies [13].

A clear effect of the cooling condition can be pointed out. Both the cryogenic machined samples stood at the highest nano-hardness values. On the contrary, dry and flood machined samples recovered more rapidly the bulk hardness. This hardness increase may be ascribed to the lower cutting temperatures in cryogenic machining that promoted a hardness rise due to the combination of decreased thermal softening and greater grain refinement than in the other cutting conditions [15].

It is worth noting that the cryogenic-machined EBM alloy is the only sample that did not totally recover the nano-hardness value of the bulk at 30 µm from the machined surface, owing to the combined effect of cryogenic machining and EBM alloy properties.

Table 3 reports the residual stresses measurements as a function of the process parameters investigated at the machined surface along the axial and tangential directions.

In all the investigated conditions, the residual stresses were compressive, according to previous research studies [5,16], which can be considered beneficial to assure high fatigue and corrosion resistance [4,5]. In literature it is stated that harder materials lead to more compressed surfaces [17]. This trend was respected in the case of axial residual stresses since for the EBM samples the absolute values were always greater than for the wrought ones at a given cooling condition, whilst the opposite trend was found for the tangential residual stresses. In all the investigated samples, the tangential residual stresses were higher than the axial ones and cryogenic cooling positively affected residual stresses since it always induced more compressed surfaces. By using liquid nitrogen, the temperature is greatly reduced during cutting, limiting the thermal component that is the responsible of the tensile state of stress. These results follow the trend already identified in the microstructural and mechanical analyses.

3.2 Machined surface topography and defects

Table 4 reports the surface texture parameters as a function of the Ti6Al4V processing route and cooling condition. The EBM samples showed higher values of both the surface roughness (*Sa*) and reduced valleys depth (*Svk*), as well as lower values of skewness (*Ssk*) in any cooling condition compared to the wrought samples. High *Svk* values are indicative of deeper valleys, whilst low *Ssk* values are indicative of higher concentration of valleys. Both the features play a role as stress concentration sites that are favorable spots for cracks onset. This may lead to a reduction of fatigue resistance that is pivotal for medical implants since they are subjected to repeated loads. It is worth noting that *Sa* and *Svk* are not always indicative parameters to describe fatigue performances of a component [10] even if it is generally recognized that the higher the surface roughness the lower the fatigue strength [18]. In this sense, it can be stated that the surface quality of machined AM samples is lower than the one of the wrought samples [11].

Table 4. Surface texture parameters as a function of the process parameters.

Processing route	Cooling condition	Sa (µm)	Svk (µm)	Ssk (-)
Wrought	Dry	0.54 ± 0.01	0.23 ± 0.04	0.48 ± 0.02
Wrought	Flood	0.51 ± 0.01	0.18 ± 0.03	0.52 ± 0.02
Wrought	Cryogenic	0.57 ± 0.01	0.18 ± 0.02	0.52 ± 0.02
EBM	Dry	0.64 ± 0.02	0.55 ± 0.10	0.27 ± 0.04
EBM	Flood	0.63 ± 0.06	0.27 ± 0.12	0.50 ± 0.06
EBM	Cryogenic	0.97 ± 0.01	0.39 ± 0.12	0.19 ± 0.03

For what concerns the wrought material, the dry condition induced the worst surface quality in terms of texture parameters. On the contrary, flood and cryogenic conditions stood at comparable values. The latter cooling conditions led to the lowest and the highest values of *Sa* respectively, being the dry machined sample in the middle. The highest value of *Sa* found for the cryogenic cooled surfaces could be related to the reduced plasticity induced by low temperatures and so to the formation of thorough grooves [4].

As regards the EBM material, the differences in surface roughness were more emphasized. *Sa* for EBM cryogenic-machined samples was approximately 54% higher than the one of the other conditions. This may be attributed to even more prominent grooves. This feature reflected also on both *Svk* and *Ssk* outputs, being higher and lower compared to the flood condition, respectively. Hence, the flood condition led to the formation of the best topographies for fatigue applications. Equivalent considerations can be made referring to corrosion resistance. In fact, a prevalence of deep and frequent valleys (high *Svk* and low *Ssk*) correlates well with decreased corrosion resistance [12].

The SEM examination of the machined surfaces displayed surface defects that were not possible to detect by the surface roughness measurements. The SEM qualitative analysis pointed out the main defects characterizing the machined surfaces (Fig. 4). In general, all the samples showed grooves, adhered material, jagged feed marks and tearing. These findings are in accordance to what reported in literature about machined surfaces defects of difficult-to-cut alloys [14,19]. No substantial differences were found between wrought and EBM samples, being these defects typical of the cutting process. On the contrary, a different effect of the cooling condition can be highlighted. The main difference among the cooling strategies was the density of defects, which was the highest for the dry-machined surfaces and the lowest for the cryogenic-machined ones, in accordance with previous studies [4,20]. However, in case of cryogenic cooling, the very low temperatures of the coolant limited the capacity of the material to deform under the tool action, leading to irregular feed marks characterized by tearing localized in its valleys. Moreover, the size of the adhered particles reduced to less than 3 µm (Fig. 4).

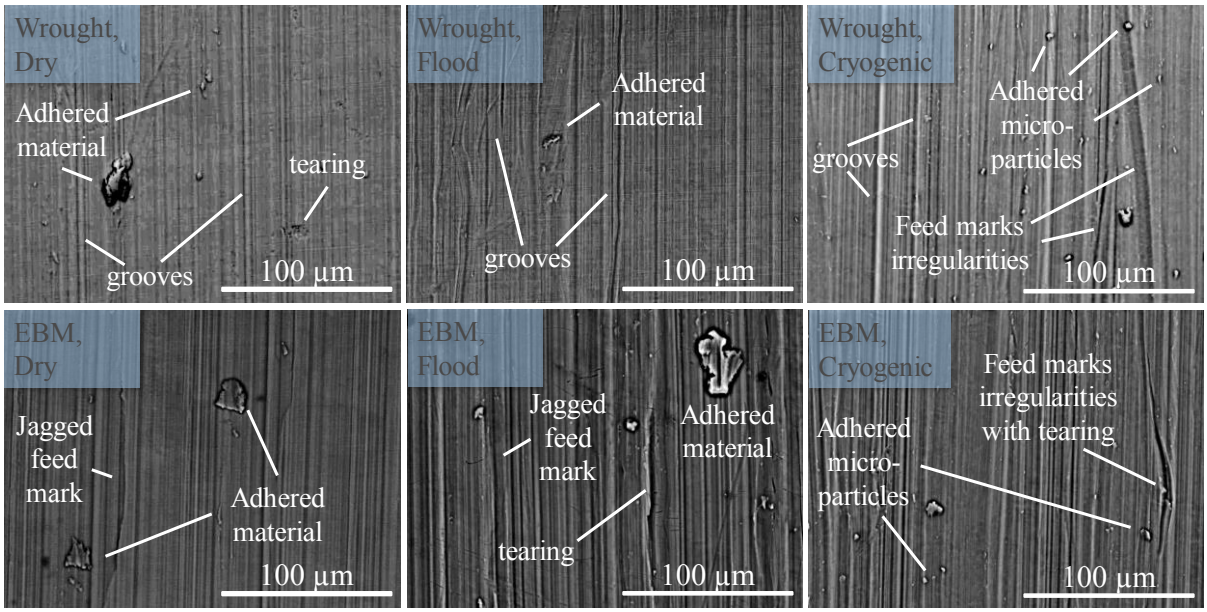

Fig. 4. SEM images in BSED mode of the turned surfaces as a function of the process parameters.

4. Conclusions

The paper investigated the surface integrity of wrought and EBM Ti6Al4V samples after finishing machining. Three different cooling techniques were employed, namely dry, flood and cryogenic. The machined surface quality was evaluated in terms of microstructural alterations (i.e. deformed layer and residual stresses), mechanical properties (i.e. nano-hardness) and surface finish (i.e. topography and defects). The principal findings of this analysis here follow:

- A machining-induced layer of higher thickness characterized the EBM samples than wrought ones. Furthermore, regardless of the processing route, cryogenic-machined samples showed a greater affected layer.
- In agreement with the microstructural alterations, EBM samples were more affected by machining in terms of nano-

hardness and axial residual stresses; cryogenic cooling provided a thicker hardened layer and more compressed surfaces.

- The main difference between the two processing routes in terms of surface integrity was appreciable when comparing the texture parameters. Regardless of the cooling condition, the EBM samples always showed the worst surface quality. Differently from the wrought condition, the cryogenic cooling did not provide an improvement in terms of surface finish, despite the benefits in terms of nano-hardness and residual stresses persisted.
- The analysis of the surface defects pointed out major differences in cooling condition rather than in alloy processing route, being the cryogenic cooled surfaces cleaner, with a smaller amount of adhered particles than the dry and flood machined ones. However, due to the lower plasticity of the material induced by the low cutting temperatures, the cryogenic-machined surfaces appeared more grooved, with irregular feed marks.

On this basis, it can be stated that the EBM Ti6Al4V alloy is surely characterized by a different machinability than the wrought one and the results of this study highlight that AM alloys need new insights for the optimization of cutting parameters.

References

[1] DebRoy T, Wei HL, Zuback JS, Mukherjee T, Elmer JW, Milewski JO, Beese AM, Wilson-Heid A, De A, Zhang W. Additive manufacturing of metallic components – Process, structure and properties. Prog Mater Sci. 2018;92:112-224.

[2] Frazier WE. Metal additive manufacturing: A review. J Mater Eng Perform. 2014;23(6):1917-1928.

[3] Jawahir IS, Brinksmeier E, M'Saoubi R, Aspinwall DK, Outeiro JC, Meyer D, Umbrello D, Jayal AD. Surface integrity in material removal processes: Recent advances. CIRP Ann - Manuf Technol. 2011;60(2):603-626.

[4] Bordin A, Sartori S, Bruschi S, Ghiotti A. Experimental investigation on the feasibility of dry and cryogenic machining as sustainable strategies when turning Ti6Al4V produced by Additive Manufacturing. J Clean Prod. 2017;142:4142-4151.

[5] Bertolini R, Bruschi S, Ghiotti A, Pezzato L, Dabalà M. Influence of the machining cooling strategies on the dental tribocorrosion behaviour of wrought and additive manufactured Ti6Al4V. Biotribology 2017;11:60-68.

[6] Titanium Consulting & Trading: wrought Ti6Al4V ELI annealed. http://www.tct.it/assets/titanium-ti6al4v-eli---annealed.pdf. [Accessed March 2019].

[7] Arcam EBM Ti6Al4V titanium alloy. http://www.arcam.com/wp-content/uploads/Arcam-Ti6Al4V-Titanium-Alloy.pdf. [Accessed March 2019].

[8] Bordin A, Bruschi S, Ghiotti A, Bariani PF. Analysis of tool wear in cryogenic turning of electron beam melted Ti6Al4V. Wear 2015;328–329:89-99.

[9] ISO 25178-2:2012 Geometrical product specifications (GPS) - Surface texture: Areal - Part 2: Terms, definitions and surface texture parameters.

[10] Dumas M, Cabanettes F, Kaminski R, Valiorgue F, Picot E, Lefebvre F, Grosjean C, Rech J. Influence of the the finish cutting operations on the the fatigue performance of Ti-6Al-4V parts produced by Selective Laser Melting. Procedia CIRP. 2018;71:429-434.

[11] Townsend A, Senin N, Blunt L, Leach RK, Taylor JS. Surface texture metrology for metal additive manufacturing : a review. 2016;46:34-47.

[12] Zecchino M. Why avarage roughness is not enough. Adv Mater Process ASM Int. 2003;161(3):25-28.

[13] Rotella G, Imbrogno S, Candamano S, Umbrello D. Surface integrity of machined additively manufactured Ti alloys. J Mater Process Technol. 2018;259(March):180-18.

[14] Ginting A, Nouari M. Surface integrity of dry machined titanium alloys. Int J Mach Tools Manuf. 2009;49(3-4):325-332.

[15] Bertolini R, Bruschi S, Ghiotti A. Large Strain Extrusion Machining under Cryogenic Cooling to Enhance Corrosion Resistance of Magnesium Alloys for Biomedical Applications. Procedia Manuf. 2018;26:217-227.

[16] Sartori S, Pezzato L, Dabalà M, Maurizi Enrici T, Mertens A, Ghiotti A, Bruschi S. Surface Integrity Analysis of Ti6Al4V After Semi-finishing Turning Under Different Low-Temperature Cooling Strategies. J Mater Eng Perform. 2018;27(9):4810-4818.

[17] Hua J, Shivpuri R, Cheng X, et al. Effect of feed rate, workpiece hardness and cutting edge on subsurface residual stress in the hard turning of bearing steel using chamfer + hone cutting edge geometry. Mater Sci Eng A. 2005;394(1-2):238-248.

[18] Grzesik W. Prediction of the Functional Performance of Machined Components Based on Surface Topography: State of the Art. J Mater Eng Perform. 2016;25(10):4460-4468.

[19] Zhou JM, Bushlya V, Stahl JE. An investigation of surface damage in the high speed turning of Inconel 718 with use of whisker reinforced ceramic tools. J Mater Process Technol. 2012;212(2):372-384.

[20] Sartori S, Bordin A, Ghiotti A, Bruschi S. Analysis of the Surface Integrity in Cryogenic Turning of Ti6Al4 v Produced by Direct Melting Laser Sintering. Procedia CIRP. 2016;45:123-126.